

Mussel shell Mn/Ca as a novel proxy for discharge in the Brazos River, Texas ~~Trace elements in mussel shells from the Brazos River, Texas: environmental and biological control~~

Authors: Alexander A. VanPlantinga¹ and Ethan L. Grossman¹

¹Department of Geology and Geophysics, Texas A&M University, College Station, Texas, USA 77843-3115

Abstract. In sclerochronology, understanding the drivers of shell chemistry is necessary in order to use shells to reconstruct environmental conditions. We measured the Mg, Ca, Sr, Ba, and Mn contents in water samples and in the shells of two freshwater mussels (*Amblema plicata* and *Cyrtonaias tampicoensis*) from the Brazos River, Texas to test their reliability as environmental archives. Shells were analyzed along growth increments using age models established with stable and clumped isotopes. Shells were also examined with cathodoluminescence (CL) microscopy to map Mn/Ca distribution patterns. In the shells, Sr/Ca correlated with Mn/Ca, while Mg/Ca and Ba/Ca showed no clear trends. Mn/Ca correlated inversely with the log of river discharge. Because [suspended chlorophyll concentration is high dissolved and inorganic particulate sources of manganese are low](#) during low flow [and suspended inorganic particles \(turbidity\) is high during high flow](#), peak Mn/Ca values may come from elevated feeding or metabolic rates [related to the abundance or suspended particulate organic matter](#). [For the first time,](#) ^sShell Mn/Ca values were used to reconstruct river discharge patterns, which, to our knowledge, has previously only been performed with shell chemistry using oxygen isotopes.

Copyright Statement

1 Introduction

Sclerochronology is the study of the physical and chemical properties of invertebrate hard parts [and the temporal context in which they grew. It is useful in marine paleoclimatology, but can also be applied to freshwater ecosystems](#). There is great potential for using mollusks to reconstruct environmental conditions in the present and in the geologic past, but problems remain in understanding the relationship between mollusk shell chemistry and the ambient environment (Immenhauser et al., 2016). For example, shell Sr/Ca can record temperature as a reflection of mollusk metabolic response to seasonal temperature variation opposite what is thermodynamically predicted for aragonite (Wheeler, 1992; Gillikin et al., 2005; Carré et al., 2006; Sosdian et al., 2006; Gentry et al., 2008). Shell Mg/Ca can record temperature (Freitas et al., 2006), and shell Ba/Ca sometimes correlates with diatom primary productivity (Vander Putten et al., 2000; Lazareth et al., 2003), but it can also be controlled by growth rate (Izumida

29 et al., 2011). Mollusk soft tissue reflects variations in metal bioaccumulation by organ and by element (Ar~~ai~~fin and
30 Bendell-Young, 2000; Chale, 2002; Ravera et al., 2003; Silva et al., 2006; Bellotto and Miecekeley, 2007). Soft
31 tissue bioaccumulation can in turn elucidate pathways to shell bioaccumulation (Puente et al., 1996; Bilos et al.,
32 1998; Langlet et al., 2007). Untangling the physical, chemical, and biological factors involved in sclerochronology
33 will improve the utility of mollusk shells as environmental archives (Vander Putten et al., 2000).

34 Studies of mollusk shell Mn/Ca have highlighted chemical, physical, and biological pathways of
35 environmental manganese, providing insight into mollusk physiology, ecosystems, food webs, and human impacts
36 such as soil erosion, eutrophication, and hypoxia (Risk et al., 2010; Langlet et al., 2007; Jacob et al., 2008; Zhao et
37 al., 2016; Zhao et al., 2017a). [Manganese is an important trace nutrient for photosynthesizers, bacteria and](#)
38 [eukaryotes, and its bioavailability is tied redox conditions and anaerobic microbial activity \(Sigeo, 2005\).](#) Aquatic
39 manganese [distribution](#), whether dissolved or particulate, is controlled by redox conditions (pH and DO), which are
40 in turn controlled by nutrient flux (Langlet et al., 2007), microbial oxidation (Sunda and Huntsman, 1990), and
41 physical factors such as wind and water currents and photoreduction (Sunda and Huntsman, 1994). Manganese can
42 be incorporated in mollusk shells via suspended organic particle ingestion (Bilos et al., 1998; Vander Putten et al.,
43 2000; Lazareth et al., 2003; Langlet et al., 2007). Dissolved Mn²⁺ is the most bioavailable form of manganese
44 (Campbell, 1995), and experimental studies using Mn-spiked water have shown the direct influence of dissolved Mn
45 on shell Mn (Jeffrey et al., 1995; Hawkes et al., 1996; Markich et al., 2002; Langlet et al., 2006; Lartaud et al.,
46 2010). Natural [variation in ~~ly~~-dissolved Mn ~~variation~~](#)-has been demonstrated to influence shell Mn/Ca in several
47 studies (Frietas et al., 2006; Barats et al., 2008; Zhao et al., 2017a). Nevertheless, little is known about the spatial
48 and temporal variation of dissolved and inorganic and organic forms of manganese, including the chemistry of river
49 colloids, sediment porewater, and phytoplankton.

50 While trace element studies of marine bivalves are common, trace element studies of freshwater mussels
51 are uncommon despite the fact that freshwater mussels are threatened worldwide by anthropogenic nutrient influxes
52 and water impoundment (Lydeard et al., 2004; Richter et al., 1997). Studies of freshwater mussel trace elements
53 have highlighted the relationship between shell metal/Ca (Me/Ca) values and water Me/Ca values (Carroll and
54 Romanek, 2008; Bolotov et al., 2015; Geeza et al., 2018), and relationships between Me/Ca and physical factors
55 such as river discharge (Risk et al., 2010) and nutrient pollution (Zhao et al., 2017a).

56 This study explores relationships between the Brazos River physical and chemical parameters and the Mg,
57 Sr, Ba, and Mn contents of freshwater mussel shells during the drought period of 2013. This work utilizes the
58 oxygen isotope sclerochronology from VanPlantinga and Grossman (2018) established with the aid of clumped
59 isotopes. This approach allows for the study of a challenging and dynamic environment, a subtropical regulated river
60 where the mussel shell isotope record cannot be tied to seasonal patterns as easily as in temperate, tropical, or
61 marine environments. Building on the water and shell isotope data, the present study focuses on trace metals and
62 their relation to river nutrients. Although the shell Sr/Ca-temperature relationship was expected (Gillikin et al.,
63 2005; Carré et al., 2006; Sosdian et al., 2006; Izumida et al., 2011), the inverse Mn/Ca-discharge relationship is a
64 novel finding. It indicates that river flow influences ~~controls~~ the bioavailability of manganese. Below we explore the
65 basis for this unusual observation and recommend further research on river manganese flux.

66 2 Methods

67 2.1 Setting, water sampling and analysis

68 This study focuses on the middle run of the Brazos River near College Station, Texas (near the USGS gage
69 08108700 in Bryan, Texas) about 210 km north of its estuary in the Gulf of Mexico (Figure 1). Water impoundment
70 near this study site negatively impacts mussel diversity (Randklev et al., 2013; Tsakiris and Randklev, 2016) in the
71 Brazos River. The Brazos flows southeast through a semi-arid to semi-humid climate characterized by hot summers
72 and mild winters, averaging 29°C and 13°C, respectively (Nielsen-Gammon, 2011). Average annual rainfall in
73 College Station is 100 cm and historically peaks in late-spring and mid-fall. About 240 km upstream of the study
74 site is Lake Whitney, dammed for hydropower and flood control. About 30 km upstream of the study site is the
75 confluence with the Little River, the largest Brazos tributary, receiving flows from Lake Belton, Stillhouse Hollow
76 Lake, and Granger Lake, all dammed reservoirs. The Brazos is noted for high turbidity during times of high
77 discharge, and, conversely, high suspended chlorophyll concentration and high rates of water column primary
78 productivity at low flow (Roach et al., 2014).

79 From January 2012 through July 2013, weekly temperature, pH measurements, and water samples were
80 collected from the Brazos River at the Highway 60 bridge between Brazos and Burleson counties (VanPlantinga et
81 al., 2017). Water samples were measured for $\delta^{18}\text{O}$ and δD using a Picarro L2120i cavity ringdown spectrometer at
82 the Stable Isotope Geoscience Facility at Texas A&M University. Calibration procedures, water $\delta^{18}\text{O}$ values

83 $(\delta^{18}\text{O}_{\text{water}})$, and temperature values are given in VanPlantinga et al. (2017). Discharge data for the Brazos River at
84 Highway 21 near College Station (USGS 08108700) were obtained online from <http://waterdata.usgs.gov/tx>.

85

86 2.2 Shell samples and analyses

87 On August 9, 2013, four specimens each of *Amblyma plicata* and *Cyrtornaias tampicoensis* were collected
88 live from the Brazos River near the Highway 60 bridge, from the sandy river bed shallower than 2 m depth. Mussels
89 were frozen, then shucked. Their shells were scrubbed, sonicated in water, and dried.

90 One specimen each of modern young adult *A. plicata* (labelled 3R5) and *C. tampicoensis* (TP3) were
91 randomly selected and analyzed. Based on stable and clumped isotope analyses, the shells are estimated to be 3-4
92 years old (VanPlantinga and Grossman, 2018). Specimens were sectioned, broken in two, and epoxied to glass
93 slides. Shell powder samples were collected with a New Wave Micromill using a 0.5 mm drill bit following the
94 methods of Dettman and Lohmann (1995). Two transects were sampled in each shell: one across the ventral margin
95 region (or VM, also referred to as the outer nacreous layer or ONL), and one across the INL region (inner nacreous
96 layer) as shown in Figure 2. Sample intervals were between 60 and 140 μm , with generally shorter spacing for INL
97 than ONL. [The shell banding patterns in the cathodoluminescence images discussed below occur on a scale of 100s](#)
98 [of \$\mu\text{m}\$ and are resolved accurately with the micromill sampling method.](#) About 60 μg per sample were reacted in a
99 Kiel IV carbonate instrument with phosphoric acid (specific gravity = 1.925 g/cm^3) and the CO_2 analyzed on a
100 Thermo Finnigan MAT253 mass spectrometer in the Stable Isotope Geosciences Facility at Texas A&M University.
101 Average analytical precision was 0.05‰ for $\delta^{18}\text{O}$ and 0.03‰ for $\delta^{13}\text{C}$.

102 For ICP-MS analysis, 20-160 μg of powder, [subsampling from the micromilled IRMS samples described](#)
103 [above](#), were completely dissolved in 2 mL of 2% nitric acid solution. [The pairing of stable isotope and trace element](#)
104 [analyses allow for precise age controls on the trace element data. Trace element ICP-MS analyses were was](#)
105 performed on a Thermo Scientific high resolution inductively-coupled plasma mass spectrometer (HR-ICP-MS) at
106 Texas A&M University's Williams Radiogenic Isotope Geosciences Laboratory for the following nuclides: ^{25}Mg ,
107 ^{43}Ca , ^{55}Mn , ^{88}Sr , ^{137}Ba , and ^{56}Fe . The USGS MACS3 coral reference standard was used as a validation standard (N =
108 12), and error analysis is provided in Table 1. An indium spike was added to all samples and standards to monitor
109 instrumental drift. ~~TP Because the water samples were also prepared with 2% nitric acid and indium spikes, but were~~
110 ~~not filtered and were acidified for analysis after months in storage.~~ [As the samples were not originally intended for](#)

111 ~~trace element analysis and sat in storage, dissolved manganese likely adsorbed to particles before acidification and~~
112 ~~analysis, so measurements of dissolved~~ Mn concentrations may be underestimated. Below, we discuss the shell
113 Mn/Ca values without relying heavily on the water measurements.

114 ~~Cathodoluminescence microscopy (CL) was used in order to map the distribution of manganese in the shell~~
115 ~~mineral lattice. After micromill samples were taken for paired geochemical analysis,~~ cross sections of TP3 and
116 3R5 shells were photographed with ~~CL~~ cathodoluminescence microscopy (CL) using a Technosyn 8200 MKII cold
117 cathode luminoscope following the methods of Roark et al. (2016). Samples were exposed to a 400 nA and 20 kV
118 beam with photograph exposure of about 30s. Photomosaics of the CL images were arranged over high resolution
119 scans of the shell cross sections and then analyzed with ImageJ software. Brightness profiles were plotted from the
120 same locations in the shells as the micro-drilled transects. Although some CL photographs had shadows in the
121 bottom left corners, shadows were cropped out in the INL regions. In order to avoid shadows in the VM regions,
122 data points in the shadows were identified on the plot in Figure 3A (corresponding to the labeled regions in Figure
123 2) and removed from the CL data set analyzed in the cross-correlation matrix (Table 2). The CL comparisons in
124 Table 2 excluded 8 points from 3R5 and 1 point from TP3 from the shadowy regions of the CL photomosaics.
125 Normalized image brightness profiles were then compared with ICP-MS results using Pearson's r values. To avoid
126 false positives with multiple comparisons, we use a Bonferroni correction for the overall level of significance α
127 (0.05), divided by 52 comparisons, resulting in significance threshold of $p < 10^{-3}$.

128 The distribution coefficient D_{Me} represents the Me/Ca in the shell relative to the water Me/Ca, where $D_{Me} =$
129 (shell Me/Ca) / (water Me/Ca). Ranges of shell D_{Mg} , D_{Mn} , D_{Ba} , and D_{Sr} values were calculated using the minimum
130 and maximum shell Me/Ca values relative to the mean water Me/Ca values for water samples taken from April to
131 August of 2013 to overlap with the growth period of the shell VM trace element data. ~~Because our water manganese~~
132 ~~concentrations are compromised, the median value (1.2 ppb) from Keeney-Kennicutt and Presley (1986) was used to~~
133 ~~estimate DMn.~~

134

135 3 Results and discussion

136 3.1 Oxygen isotopes

137 Stable isotope growth chronologies for specimens 3R5 and TP3 are shown in Figure 3 and explained in
138 detail in VanPlantinga and Grossman (2018). ~~To develop these chronologies, we measured water temperature (T)~~

139 and $\delta^{18}\text{O}_{\text{water}}$ to predict shell $\delta^{18}\text{O}$ according to equations 1, 2, and 3 (Dettman et al., 1999, based on Grossman and
140 Ku, 1986):

141
$$1000 \ln(\alpha_{\text{aragonite/water}}) = 2.559 \times (10^6 \times T^{-2}) + 0.715 \quad (1)$$

142
$$\alpha_{\text{aragonite/water}} = \frac{(1000 + \delta^{18}\text{O}_{\text{aragonite}})_{\text{VPDB}}}{(1000 + \delta^{18}\text{O}_{\text{water}})_{\text{VSMOW}}} \quad (2)$$

143
$$\alpha_{\text{VSMOW/VPDB}} = 1.0309 \quad (\text{Gonfiantini et al., 1995}). \quad (3)$$

144 Because winter hiatuses and erratic summer growth patterns result in chaotic shell $\delta^{18}\text{O}$ patterns that complicate
145 $\delta^{18}\text{O}$ sclerochronology, we used clumped isotope thermometry to supplement $\delta^{18}\text{O}$ data (VanPlantinga and
146 Grossman, 2018).

147 Based on our shell chronology, the time interval represented by the trace element analyses is April to
148 August 2013. During this interval water temperature and $\delta^{18}\text{O}_{\text{water}}$ values ranged from 13 to 34°C and -2.7 to 1.3‰,
149 respectively. Daily averaged river discharge at the study site was 173-2230 cfs (cubic feet per second; USGS gage
150 08108700; <https://waterdata.usgs.gov>). The higher $\delta^{18}\text{O}_{\text{water}}$ values reflect increased summer evaporation combined
151 with increased proportion of flow from evaporated ^{18}O -enriched Lake Whitney water, whereas lower values (as low
152 as -8‰) are the result of ^{18}O -depleted precipitation and runoff (Chowdhury et al., 2010; VanPlantinga et al., 2017).

153 3.2 Water chemistry

154 Mean water Me/Ca values are presented in Table 1. Water dissolved ion concentration and electrical
155 conductivity results are shown in Figures 4A and 4B. The Sr, Ca, and Ba results correlate track with the electrical
156 conductivity ($p < 0.05$) because Brazos River salinity is strongly controlled by the proportion of river flow
157 discharged from Lake Whitney (Chowdhury et al., 2010; VanPlantinga et al., 2017). The correlation between Mg
158 and Ca (Figure 4B) is due to the dominance of Mg²⁺ and Ca²⁺ over Na⁺, Sr²⁺, and Ba²⁺, and Cl⁻ in the runoff and
159 bank storage water source endmember (VanPlantinga et al., 2017; Rhodes et al., 2017). Brazos River Alluvium
160 Aquifer (BRAA) influence is strongest in the hours after strong rain (Rhodes et al., 2017), and so manganese-
161 scavenging particles in the high-Ca²⁺-Mg²⁺-HCO₃⁻ samples probably explains the inverse Ca-Mn correlation in
162 our unfiltered water samples, where manganese carbonates are favored. Mg, Sr, and Ba correlated positively with Ca
163 concentrations and Mn correlated negatively with Ca ($R_{\text{sq}} > 0.55$, $p < 0.0007$). Water Mn/Ca, Ba/Ca, and Sr/Ca
164 values (mmol/mol) significantly correlate with each other ($p < 0.00011$), and further, Mg/Ca weakly correlates with

Formatted: Indent: Left: 0", Space After: 0 pt, Border: Top: (No border), Bottom: (No border), Left: (No border), Right: (No border), Between : (No border)

Formatted: Space After: 0 pt, Border: Top: (No border), Bottom: (No border), Left: (No border), Right: (No border), Between : (No border)

Commented [1]: needs clarification, relationships are confusing

Commented [2]: Electrical conductivity, as a proxy for LW influence, does not show a relationship with water Mn(ppb), the p value is 0.57, rsq = -0.04.

Commented [3]: _Marked as resolved_

Commented [4]: _Re-opened_

165 Sr/Ca and Ba/Ca ($p < 0.015$). USGS data for the Brazos River gage at Bryan, Texas (08108700) generally display an
166 inverse relationship between dissolved oxygen and discharge. On a linear scale, the element with the highest
167 concentration, calcium, showed the greatest variation (19–83 ppm), but on a log scale magnesium concentration
168 showed the most variation (12 ppb–20 ppm; Figure 4). While the low measured water manganese concentrations
169 (0.1–0.6 ppb) are consistent with Keeney-Kennicutt and Presley's (1986) measurements of Brazos River water (0.1–
170 2.3 ppb), but we will not draw conclusions based on the water Mn data because our water samples were not filtered
171 after and acidified immediately upon collection, so true dissolved Mn²⁺ from the time of sampling cannot be
172 discussed. Turekian and Scott (1967) attribute the suspended particulate manganese concentration in the Brazos
173 River (690 ppm) to soil erosion, as found in other river Mn studies (e.g., Shiller, 2002; Risk et al., 2010). The
174 highest water Mn concentration values in our study were from samples taken during times of high flow.

175 3.3 Shell chemistry

176 Table 2 explores relationships between environment, shell growth, and shell chemistry using Pearson's r
177 values. Me/Ca values and distribution coefficients (D_{Me}) can differ between specimens 3R5 and TP3, and between
178 the ventral margin (VM) and inner nacreous layer (INL) of the same shell, especially with regard to Mg/Ca and
179 Mn/Ca (Table 1). Nevertheless, taken as a whole, the ranges in values are generally similar to those recorded in
180 previous studies of freshwater mussels (Carroll and Romanek, 2008; Geeza et al., 2018 and references cited therein),
181 except for Mg/Ca (Table 3). In addition, log of shell D_{metal} values overlap with the results in Bolotov et al. (2015) for
182 metal/calcium partitioning in *Margaritifera*, except that their Mg/Ca values are 1–4 orders of magnitude lower than
183 ours (0.001–0.11538).

184 Mg/Ca does not show any systematic patterns in our water data (Figure 3A), nor are there any
185 systematic temporal variations in the Mg/Ca or Ba/Ca values in the shells, with erratic fluctuations over several
186 orders of magnitude over the time period studied (Figures 3B and 3D4B). In terms of Furthermore, taxonomic
187 differences can be important. For example, Mg/Ca values of 3R5 are about three times greater than those of TP3.

188 Previous studies of Mg/Ca and Sr/Ca indicate that shell trace elements may be heterogeneously distributed
189 in the shell mineral lattice and organic matrix depending on ontogenetic age, ultrastructure, and crystal fabric
190 (Schöne et al., 2011; Schöne et al., 2013). Brazos River water Mg/Ca is about half that in the Scioto River in Ohio
191 (Geeza et al., 2018), but our average shell Mg/Ca values are nearly an order of magnitude higher, resulting in

Commented [5]: can we still give a rough D(Mn/Ca) estimate combining our shell data with the median of their published data (0.1–2.3ppb)???

Commented [6]: _Marked as resolved_

Commented [7]: _Re-opened_

Commented [8]: confusing. Contradicts Figure 3B

192 significantly higher D_{Mg} estimates, than in the Ohio *Lamellis cardium* shells. Differences in species or climate may
193 account for the variation in freshwater mussel D_{Mg} values.

194 As shown in Table 3, shell Ba/Ca in the ventral margin (45-2748 mg/kg) and DBa values (0.06-0.47) overlap
195 with the range reported in past studies (Carrol and Romanek, 2008; Izumida et al., 2011; Bolotov et al., 2015; Geeza
196 et al., 2017). Previous authors have linked shell Ba/Ca to diatom productivity patterns (Vander Putten et al., 2000;
197 Lazareth et al. 2003). In the absence of periodic diatom blooms, Izumida et al. (2011) attributed their lacustrine mussel
198 shell Ba/Ca to growth rate. Our data do not point to a clear physical or physiological explanation for shell Ba/Ca
199 patterns in the Brazos River specimens.

200 Ventral margin Sr/Ca and Mn/Ca correlates significantly ($p < 0.05$) with Mn/Ca in both shells. If Bonferroni
201 corrections are not used as in other studies (e.g., Vander Putten et al., 2000; Gentry et al., 2008; Izumida et al., 2011;
202 Geeza et al., 2017), all but one Sr/Ca relationship in Table 2 (with growth rate in 3R5) may be significant ($p < 0.05$),
203 corroborating the common observation that Sr/Ca correlates positively with temperature in aragonitic mollusk shells
204 (e.g., Gillikin et al., 2005; Carré et al., 2006; Sosdian et al., 2006). The Sr/Ca-temperature relationship was observed
205 in lacustrine mussels by Izumida et al. (2011), but was not observed in freshwater mussels from Ohio (Geeza et al.,
206 2018) where there was significant shell-water Sr/Ca relationship. The D_{Sr} values from the Brazos shell ventral margin
207 regions (0.08-0.19) overlap with D_{Sr} values reported in several previous studies (Carroll and Romanek, 2008; Bolotov
208 et al., 2015; Geeza et al., 2017) as shown in Table 3.

209 In terms of variation within and between shells, Sr/Ca is only slightly more concentrated in the INL than the
210 VM in both specimens. Figure 43A illustrates the similar patterns between Mn/Ca, CL brightness, shell growth rate,
211 Sr/Ca, and $\delta^{13}C$. There is a robust relationship between Sr/Ca and Mn/Ca in both the TP3 and 3R5 ventral margins
212 (Figure 3E). Sr/Ca values are similar between the two specimens, (Figure 4, Table 1).

213 As shown in Table 3 shell Ba concentrations in the ventral margin (45-2748 mg/kg) overlap with the range
214 reported in past studies (Carrol and Romanek, 2008; Bolotov et al., 2015; Geeza et al., 2017). Brazos shell D_{Ba} values
215 (0.06-0.47) overlap with values given in other studies of freshwater mussels (Izumida et al., 2011; Bolotov et al., 2015;
216 Geeza et al., 2017). Out of the four Me/Ca parameters, Ba/Ca showed the second lowest mean values in the water and
217 in the shells. Ba/Ca values overlap with the range reported in past studies (Table 1; Carrol and Romanek, 2008;

Formatted: Justified, Space Before: 12 pt, After: 12 pt

218 Bolotov et al., 2015; Geeza et al., 2017). Ba/Ca are 29% higher in the Tampico specimen (TP3) than the three ridge
219 specimen (3R5). Ba/Ca was higher in the Tampico VM region than in the INL, but higher in the three ridge INL than
220 the VM.

221 While water Ba concentration is likely driven by the proportion of flow from Lake Whitney discharge, as
222 with Sr, Mg, and Ca (Chowdhury et al., 2010; VanPlantinga et al., 2017), the shell Ba/Ca values do not show any
223 systematic patterns. Previous authors have linked shell Ba/Ca to diatom productivity patterns (Vander Putten et al.,
224 2000; Lazareth et al. 2003). In the absence of periodic diatom blooms, Izumida et al. (2011) attributed their lacustrine
225 mussel shell Ba/Ca to growth rate. Our data do not point to a clear physical or physiological explanation for shell
226 Ba/Ca patterns in the Brazos River specimens.

Commented [9]: condense the Mg, Sr, and Ba discussion

227 —Shell ONL Mn/Ca values (mmol/mol) are shown in Figure 34A. Shell Mn concentrations (67-2308 mg/kg)
228 overlap with ranges reported in several studies (Nyström et al., 1996; Mutvei and Westermarck, 2001; Markich et al.,
229 2002; Verdegaal, 2002; Ravera et al., 2003; Langlet et al., 2007; Carroll and Romanek, 2008; Bolotov et al., 2015;
230 Zhao et al., 2017a; Geeza et al., 2017). The D_{Mn} values from the shell ventral margin regions in this study (13-2284)
231 overlap with D_{Mn} ranges reported in Geeza et al. (2018) and Bolotov et al. (2015) but are much higher than other
232 studies where $D_{Mn} < 1$ (Markich et al., 2002; Verdegaal, 2002; Carroll and Romanek, 2008). The average D_{Mn} values
233 of the 3R5 and TP3 INL regions are higher (~42-6380-200). Compared to thermodynamic predictions for abiogenic
234 aragonite, biogenic aragonite has relatively high substitution rates of Mn^{2+} for Ca^{2+} in the mineral lattice (Soldati et
235 al., 2016). Relatively high D_{Mn} values (>10) in biogenic aragonite, as reported here, suggest a physiological process
236 of concentrating Mn^{2+} during biomineralization. The influence that factors such as species differences, environment,
237 and ontogeny have on D_{Mn} remain to be determined.

238 Mn/Ca values are significantly higher and more variable in the INL than VM (or ONL) regions in both
239 TP3 and 3R5 specimens (Table 1). Figure 4B shows shell INL Mn/Ca and water Mn/Ca for 2012-2013. Siegele et al.
240 (2001) suggested that shell growth rings have elevated manganese and organic matter content in *Hyridella depressa*,
241 and they inferred different shell chemistry and mineralization processes between the shell umbo and ventral margin.
242 Carroll and Romanek (2008) suggest that differences between INL and ONL trace element values may come from
243 higher rates of dissolution and reprecipitation in the INL than in the ONL. Oeschger (1990) suggested that anaerobiosis
244 contributes to the internal dissolution of the shell in *Arctica islandica*. Some biomineralization models indicate that

245 the INL is exposed to extrapallial fluid of a different chemical composition than the EPF in contact with the shell ONL
246 region (Schöne and Krause, 2016). If this is the case, then the shell INL trace element values may be less appropriate
247 for some environmental reconstruction than the ONL region. Higher Mn/Ca in the INL than in the VM regions of the
248 Brazos River specimens suggests indicates physiological influence control on the distribution of Mn in the shell.
249 Mn/Ca and Ba/Ca values are on average ~3027% higher in the Tampico specimen (TP3) than the threeridge specimen
250 (3R5). This may reflect species or individual differences in physiology or behavior metabolic rate or feeding.

251 Shell ONL Mn/Ca correlates inversely with log of river discharge ($p < 0.05$, Table 2), allowing for the
252 reconstruction of times of high and low flow. Figure 4F reconstructs trends in log of Brazos River discharge
253 ($\log_{10}Q$) from Mn/Ca in TP3 ($\log_{10}Q = -1.11 \times \text{Mn/Ca}_{\text{shell}} + 3.17$) and in 3R5 ($\log_{10}Q = -1.22 \times \text{Mn/Ca}_{\text{shell}} + 2.99$).
254 The reconstruction is more accurate in the summer but overestimates observed discharge in the spring, possibly due
255 to seasonal changes in water Mn/Ca or biological controls on shell Mn/Ca. Because of 1) the higher Mn/Ca in the
256 INL relative to the VM regions in the shells, and 2) the strong relationship between shell Mn/Ca and river discharge,
257 we infer both physical and biological controls on shell Mn/Ca, as discussed below.

258 Previous studies have used shells chemistry to reconstruct river discharge such as by linking high runoff
259 events to elevated suspended Mn from soil erosion (Risk et al., 2010). Many sclerochronological reconstructions of
260 discharge are based on stable oxygen isotopes (Mueller-Lupp et al., 2003; Dettman et al., 2004; Versteegh et al., 2011;
261 Ricken et al., 2003; Kelemen et al., 2018). Our study indicates that either Brazos River mussel activity patterns
262 (physiological or behavioral feeding and/or metabolic rate), or water source and chemistry, are influenced by
263 discharge rates and that these variations are recorded in the trace element composition, particularly Mn/Ca, of the shell
264 mineral. Here we reconstruct river discharge variation and distinguish times of low and high flow using shell Mn/Ca
265 values (Figure 3F).

266 3.4 Cathodoluminescence

267 Cathodoluminescence (CL) is a common tool for mapping the distribution of manganese in biogenic
268 carbonates (Barbin, 2000). Lattice-bound Mn caused greenish-yellow luminescence under CL on a sub-mm scale
269 similar to the spatial resolution of micromilled chemical samples. The CL images reveal alternating bright green-
270 yellow and dim banding that generally correlates with the pattern of light and dark banding in plane light (Figure 2).

271 The results verify that the Mn is lattice-bound (Table 2) and reveal the complex cyclicity of Mn distribution in the
272 shell (Lartaud et al., 2009). CL brightness also weakly correlates with Sr/Ca and G (growth rate) in both shells.

273 3.5 Dissolved and particulate sources of Mn

274 Manganese incorporated into the mussel shells may be derived from dissolved Mn²⁺ or ingested particulate
275 Mn. Several factors affect manganese concentration and flux in the environment. Reducing conditions, low DO, and
276 low pH increase manganese solubility (Tebo et al., 2004). Microbial activity combined with high nutrient flux and
277 low rates of water column mixing can cause hypoxia, reducing conditions, and elevated dissolved Mn²⁺
278 concentration (Zhao et al., 2017a). Other factors influencing Mn availability include photo-inhibition of Mn²⁺-
279 oxidizing bacteria, reductive dissolution from sunlight (Sunda and Huntsman, 1994), primary production, benthic
280 decomposition, algal uptake of dissolved Mn²⁺ (Sunda and Huntsman, 1985), and influx of allochthonous dissolved
281 Mn²⁺ (Langlet et al., 2007).

282 Shell manganese could be influenced by point sources such Lake Whitney or the Little River. ~~Lake
283 Whitney and Little River manganese concentrations are near the mean values of the Brazos River (-0.2ppb in this
284 study). Lake Whitney has periodic brown algae blooms (Roelke et al., 2011). However, if Lake Whitney was the
285 driver of shell Mn/Ca patterns, then the water Mn concentration would correlate with electrical conductivity, Sr
286 concentration, and Ba concentration, but does not (p > 0.05)/Ca patterns would not be inversely related to water
287 Sr/Ca, Ba/Ca, and Mg/Ca. Lake Whitney experiences a fall overturn where manganese and iron-rich oxygen
288 depleted water mixes with the overlying water column (Strause and Andrews, 1984), but the temperature and water
289 chemistry changes in the spring and summer are typically more gradual. Hydroelectric releases from the Whitney
290 dam flow from 7 meters above lake bottom. The hypothesis that seasonal stratification patterns in Lake Whitney,
291 240 km away, drive downstream mussel shell Mn/Ca variation in the spring is not supported. Elevated δ¹³C in the
292 shells during the summer of 2013 was interpreted as an indication of heightened Lake Whitney influence on river
293 flow and chemistry during drought conditions (VanPlantinga and Grossman, 2018; VanPlantinga et al., 2017). There
294 is a correlation between δ¹³C and Mn/Ca in 3R5 but not in TP3. There is not yet sufficient evidence to indicate that
295 Lake Whitney or the Little River are point sources of shell manganese, nor to explain the striking inverse shell
296 Mn/Ca - river discharge relationship, but ~~this does not diminish the point source hypothesis cannot be ruled out~~~~

Commented [10]: water Mn/Ca positively correlates with water Sr/Ca and Ba/Ca but not Mg/Ca

Commented [11]: there is no relationship between river Ca(ppb) and ECond

Commented [12]: If this is the argument for Mn source, then it must be plotted

297 ~~given~~ the important role Lake Whitney plays in ~~downstream river-major dissolved ion~~ chemistry ~~downstream~~
298 (VanPlantinga et al., 2017).

299 Dissolved Mn²⁺ is the most bioavailable form of manganese (Campbell, 1995). Shell Mn/Ca values have
300 been attributed to variations in dissolved Mn²⁺ in the water column (Frietas et al., 2006; Barats et al., 2008) and in
301 the sediment porewater (Zhao et al., 2017a). As mentioned earlier, experimental studies have confirmed that
302 dissolved Mn²⁺ content is recorded in shell Mn/Ca (Jeffree et al., 1995; Hawkes et al., 1996; Markich et al., 2002;
303 Langlet et al., 2006; Lartaud et al., 2010). However, the low dissolved oxygen conditions in the Brazos River, which
304 should ~~increase the concentration of favor high~~ dissolved Mn²⁺, occur at times of high flow (USGS 08108700 gage
305 data ~~from waterdata.usgs.gov~~) when shell Mn/Ca is relatively low. ~~These data related to r~~Redox conditions in the
306 water column do not explain the shell Mn/Ca patterns, and we lack the data to evaluate the hypotheses that
307 sediment porewater drives shell Mn/Ca, ~~or if HCO₃--rich bank water favors the precipitation of dissolved Mn²⁺ out~~
308 ~~of solution in the days following heavy rainfall. These hypotheses should be explored in future studies.~~

309 Particulate Mn, bound to organic or inorganic particles, can also be a source of Mn in shells. The inverse
310 relationship between water Ca and Mn concentrations (Figure 4B) indicates that Mn ~~solubility flux into the water~~
311 may be related to runoff ~~and rapidly discharged bank storage~~ from local rain storms (Rhodes et al., 2017), ~~in contrast~~
312 ~~to the Ca sourced from the upstream reservoir Lake Whitney (Chowdhury et al., 2010; VanPlantinga et al., 2017).~~
313 Bilos et al. (1998) attributed elevated clam soft tissue Mn to higher turbidity and ingestion of Mn-bearing inorganic
314 particles. Because Mn/Ca is inversely correlated with log of discharge in this study, inorganic particles (suspended
315 during at times of high flow) are probably not the source of Brazos River mussel shell Mn/Ca.

316 Previous studies have attributed bivalve shell Mn/Ca to ingestion of Mn-bearing organic particles such as
317 phytoplankton. Vander Putten et al. (2000) and Lazareth et al. (2003) found significant shell Ba/Ca-Mn/Ca
318 correlations in estuarine bivalves indicative of diatom ingestion. Brazos River phytoplankton are typically not
319 diatoms (Roelke, personal communication) and there is no shell Ba/Ca-Mn/Ca relationship in our data. Geeza et al.
320 (2018) examined oxygen, chlorophyll, and pH as a proxy for primary productivity (based on Goodwin et al., 2018),
321 but did not find correlations with shell Mn/Ca. Nevertheless, they ~~did not discount the possibility could not rule out a~~
322 ~~that~~ phytoplankton or microbial manganese reduction (Lovley and Phillips, 1988) influences ~~on their~~ shell Mn/Ca
323 values.

Commented [13]: check the absolute concentration of Ca in LW and BR

324 Roach et al. (2014) found elevated chlorophyll concentrations in the Brazos River near our study site at
325 times of low discharge in 2010-2012, with suspended chlorophyll concentration significantly higher than benthic
326 chlorophyll (40-50 mg/L₃ compared to ~11 mg/L₂), and about 5-10 times higher than the other rivers in their study.
327 Roach (2013) attributed river chlorophyll abundance to lengthened residence time, emphasizing that sediment
328 scouring and turbidity from high discharge limit phytoplankton growth (Wissmar et al. 1981; Steinman and
329 McIntire, 1990). River mussels have been observed to preferentially inhabit refugia with low rates of shear stress
330 (Layzer and Madison, 1995; Strayer, 1999; Howard and Cuffey, 2003). This may correspond to elevated manganese
331 concentrations in sediment porewater as in Zhao et al. (2017a). However, little is known about the spatial and
332 temporal variation and chemical composition of Brazos River phytoplankton, suspended load, and colloids in the
333 flowing river water and the sediment porewater. Future work should characterize these variables, as manganese is an
334 important nutrient for primary producers and, by extension, river food webs in general. This would help characterize
335 the flux of manganese in river ecosystems.

336 3.6 Manganese accumulation in shells

337 Shell Mn/Ca is potentially determined by a combination of environmental chemistry (e.g., water and
338 particle chemistry), physical conditions (e.g., temperature and discharge), and the behavior of the organism (e.g.,
339 feeding rate, growth rate, and reproductive investment). Zhao et al. (2017b) offer a similar interpretation of
340 *Corbicula fluminea* shell Ba/Ca based on laboratory experiments. In terms of feeding behavior, mussels selectively
341 ingest organic matter during filter feeding (Hawkins et al., 1996). Zhao et al. (2017a) propose that manganese
342 bioaccumulation in lacustrine mussels is enhanced by deposit feeding (Vaughn and Hakenkamp, 2001; Cahoon and
343 Owen, 1996). The elevated concentrations of suspended chlorophyll relative to benthic chlorophyll at our study
344 location at times of low flow are conditions favorable for suspension feeding (Roach et al., 2014). The propensity in
345 river mussels to inhabit refugia with minimal shear stress (Layzer and Madison, 1995; Strayer, 1999; Howard and
346 Cuffey, 2003) supports the hypothesis that Brazos River mussels thrive under conditions of low discharge with high
347 concentrations of suspended particulate organic matter to feed on.

348 It is important to consider the physiological processes and soft tissues potentially involved in manganese
349 bioaccumulation. Langlet et al. (2007) suggest that soft tissues concentrate Mn derived from the digestion and
350 absorption of organic particles and this may lead to elevated Mn/Ca values in the shells. Acidic pH in the gut makes

351 ingested particulate Mn bioavailable so that it can then accumulate in mollusk soft tissue and the shell (Arifin and
352 Bendell-Young, 2000; Owen, 1996). Nott and Nicolaidou (1993) found that a substantial 67% of ingested manganese
353 is not recovered in feces of the mollusk *Nussarius rericulatus*, and therefore it is absorbed through the digestive tract.
354 Mollusk bioaccumulation of heavy metals through the gills and digestive glands is well documented and supports the
355 hypothesis that shell manganese can bioaccumulate via food ingestion (Domouhtsidou et al., 2000; Dimitriadis et al.,
356 2003; Einsporn and Koehler, 2008).

357 The shell Sr/Ca-Mn/Ca may indicate a relationship between metabolic rate, inferred from Sr/Ca, and feeding
358 rate, inferred from Mn/Ca. Metabolic rate is influenced by factors such as ontogeny, reproductive investment,
359 environmental stress (drought, flood, predation), and seasonal feeding patterns (Bayne et al., 1989). Brazos mussel
360 shell Sr/Ca may reflect metabolic patterns that cause varying rates of ion transport into the EPF as hypothesized in
361 Carré et al. (2006). Zhao et al. (2016) experimentally changed dissolved Ca^{2+} concentrations and used lanthanum and
362 Verapamil to artificially inhibit Ca^{2+} channels in the freshwater bivalve *Corbicula fluminea* and concluded that Mn^{2+}
363 and Ca^{2+} compete to cross ion channels during biomineralization. In light of the important role ion channels play in
364 biomineralization, the Sr/Ca-Mn/Ca correlation in the Brazos River shells points to a relationship between metabolic
365 rate and feeding rate. However, the physiological mechanism of ion channels does not necessarily diminish the
366 importance of environmental factors such as water chemistry and redox conditions in determining shell Me/Ca values,
367 as indicated in many studies (Campbell, 1995; Jeffree et al., 1995; Hawkes et al., 1996; Markich et al., 2000; Frietas
368 et al., 2006; Langlet et al., 2006; Barats et al., 2008; Lartaud et al., 2010; Zhao et al., 2017a; and for Sr/Ca in the case
369 of Geeza et al., 2017).

370 Little is known about the pathway that environmental manganese takes from ingestion to shell mineralization.
371 Amorphous calcium carbonate (ACC), conveyed by hemocytes to the mantle, is the precursor to the shell mineral
372 (Addadi et al., 2003; Mount et al., 2004; Li et al., 2016). The ACC has higher Mn and other metal concentrations than
373 the shell mineral (Thomson et al., 1985; Jacob et al., 2008). Initial manganese exposure may be primarily to the gills,
374 hemolymph, mantle, or digestive tract, and it may travel to the site of biomineralization via particulate or dissolved
375 forms through the hemolymph and mantle tissue. Marin et al. (2012) describe intercellular and intracellular dissolution
376 and formation of ACC granules in the mantle tissue, potentially blurring the distinction between granule and calcium

377 ion channel transport of trace metals to be incorporated into the shell mineral lattice. Dissolved and ACC-bound Mn²⁺
378 physiological pathways should be investigated further.

379 **5 Conclusions**

380 Mn/Ca values for Brazos River mussel shells showed a cyclical pattern revealed by time series analyses
381 and cathodoluminescence, which maps a pattern similar to the growth bands. Mn/Ca correlated inversely with log of
382 discharge, allowing for a reconstruction of river discharge patterns during the study period. Mn/Ca is likely
383 influenced by ingestion rates of Mn-bearing suspended particulate organic matter because shell Mn/Ca is high when
384 river discharge and turbidity are low, ruling out inorganic particles as the control on shell Mn/Ca. The shell Mn-Sr
385 relationship and the evidence of high suspended chlorophyll at times of low flow (~~Reach et al., 2014~~) point to
386 elevated metabolic activity and likely increased feeding rate in response to food abundance, and possibly lower
387 shear stress and turbidity, at times of low flow. Future research on shell and water chemistry should: 1) further the
388 scientific understanding of river plankton; 2) spatial and temporal variation in suspended colloidal and sediment
389 porewater manganese concentrations variation; and 3) elucidate ~~resolve~~ taxonomic D_{Mn} differences; ~~and 4) elucidate~~
390 elucidate specifically why different mussels in different environments have D_{Mn} values <1 ~~and while others have~~
391 D_{Mn} values ~~are~~ >10.

392

393 **Code/Data Availability**

394 Data are available on earthchem.org.

395 **Authors' Contributions**

396 A. VanPlantinga collected and analyzed data, made plots and tables, and wrote and revised the manuscript. E.

397 Grossman provided funding and edited the manuscript, the plots, and the tables.

398 **Competing Interests**

399 The authors have no competing interests to declare.

400 **Acknowledgments**

401 The authors would like to thank the Michel T. Halbouty Chair in Geology at Texas A&M University for
402 supporting this research. Luz Romero, Franco Marcantonio, and the Texas A&M AgriLife Extension Soil, Water
403 and Forage Testing Laboratory analyzed shell and/or water samples. Charles Randklev and Eric Tsakiris collected
404 the mussel specimens. Ann Molineux from The University of Texas Jackson School Museum of Earth History
405 provided historical specimens from the Singley-Askew Collection. Charles Randklev and Robert G. Howells
406 provided helpful perspective on mussel ecology. Ben Passey, Naomi Levin, Huanting Hu, Haoyuan Ji, Sophie
407 Lehmann, Dana Brenner, and Lai Ming provided valuable assistance at the Johns Hopkins University Stable Isotope
408 Lab. Chris Maupin, Lauren Graniero, Andrew Roark, and Brendan Roark helped run isotope samples at the Stable
409 Isotope Geoscience Facility at Texas A&M University. Clumped isotope analyses were financed by NSF grant
410 EAR-1226918. Data reported here are in the following online repository: earthchem.org. We thank [the](#) reviewers
411 [Christopher Romanek and David Dettman](#) for their helpful comments.

412 **References**

- 413 Addadi, L., Raz, S. and Weiner, S.: Taking advantage of disorder: amorphous calcium carbonate and its roles in
414 biomineralization. *Advanced Materials*, 15(12), pp.959–970, 2003.
- 415 Arifin, Z. and Bendell-Young, L.I.: Influence of a selective feeding behaviour by the blue mussel *Mytilus trossulus*
416 on the assimilation of ¹⁰⁹Cd from environmentally relevant seston matrices. *Marine Ecology Progress*
417 *Series*, 192, pp.181–193, 2000.
- 418 Barats, A., Amouroux, D., Pécheyran, C., Chauvaud, L. and Donard, O.F.X.: High –
419 frequency archives of manganese inputs to coastal waters (Bay of Seine,
420 France) resolved by the LA–ICP–MS analysis of calcitic growth layers along
421 scallop shells (*Pecten maximus*). *Environmental Science & Technology*, 42(1), pp.86–92, 2007.
- 422 Barbin, V.: Cathodoluminescence of carbonate shells: biochemical vs diagenetic process, in *Cathodoluminescence*
423 *in Geosciences*, edited, pp. 303–329, Springer, 2000.
- 424 Bayne, B.L., Hawkins, A.J.S., Navarro, E. and Iglesias, I.P.: Effects of seston concentration on feeding, digestion
425 and growth in the mussel *Mytilus edulis*. *Marine Ecology Progress Series*, pp.47–54, 1989.
- 426 Bellotto, V.R. and Miekeley, N.: Trace metals in mussel shells and corresponding soft tissue samples: a validation
427 experiment for the use of *Perna perna* shells in pollution monitoring. *Analytical and Bioanalytical*
428 *Chemistry*, 389(3), pp.769–776, 2007.
- 429 Bilos, C., Colombo, J.C. and Presa, M.J.: Trace metals in suspended particles, sediments and Asiatic clams
430 (*Corbicula fluminea*) of the Río de la Plata Estuary, Argentina. *Environmental Pollution*, 99(1), pp.1–11,
431 1998.
- 432 Bolotov, I.N., Pokrovsky, O.S., Auda, Y., Bepalaya, J.V., Vikhrev, I.V., Gofarov, M.Y., Lyubas, A.A., Viers, J.
433 and Zouiten, C.: Trace element composition of freshwater pearl mussels *Margaritifera* spp. across Eurasia:
434 testing the effect of species and geographic location. *Chemical Geology*, 402, pp.125–139, 2015.

- 439 [Cahoon, L.B. and Owen, D.A.: Can suspension feeding by bivalves regulate phytoplankton biomass in Lake](#)
440 [Waccamaw, North Carolina?. *Hydrobiologia*, 325\(3\), pp.193-200, 1996.](#)
- 441 Carré, M., Bentaleb, I., Bruguier, O., Ordinolà, E., Barrett, N.T. and Fontugne, M.: Calcification rate influence on
442 trace element concentrations in aragonitic bivalve shells: evidences and mechanisms. *Geochimica et*
443 *Cosmochimica Acta*, 70(19), pp.4906–4920, 2006.
- 444 Carroll, M., and Romanek, C. S.: Shell layer variation in trace element concentration for the freshwater bivalve
445 *Elliptio complanata*, *Geo-Marine Letters*, 28(5-6), 369–381, doi:10.1007/s00367-008-0117-3, 2008.
446
- 447 Chale, F.M.M.: Trace metal concentrations in water, sediments and fish tissue from Lake Tanganyika. *Science of the*
448 *Total Environment*, 299(1–3), pp.115–121, 2002.
449
- 450 Chowdhury A, Osting T, Furnans J, Mathews R.: Groundwater–surface water interaction in the Brazos River Basin:
451 evidence from lake connection history and chemical and isotopic compositions: Texas Water Development
452 Board Report, 375 (August):1–61, 2010.
453
- 454 Dettman, D. L., and Lohmann, K. C.: Microsampling carbonates for stable isotope and minor element analysis:
455 Physical separation of samples on a 20 micrometer scale: *Journal of Sedimentary Research*, 65(3), 1995.
456
- 457 [Dettman, D. L., Reische, A. K. and Lohmann, K.C.: Controls on the stable isotope composition of seasonal-growth](#)
458 [bands in aragonitic fresh-water bivalves \(Unionidae\), *Geochimica et Cosmochimica Acta*, 63\(7\), 1049–](#)
459 [1057, 1999.](#)
- 460
- 461 Dettman, D. L., K. W. Flessa, P. D. Roopnarine, B. R. Schöne, and Goodwin, D. H.: The use of oxygen isotope
462 variation in shells of estuarine mollusks as a quantitative record of seasonal and annual Colorado River
463 discharge, *Geochimica et Cosmochimica Acta*, 68(6), 1253–1263, 2004.
464
- 465 Dimitriadis, V.K., Domouhtsidou, G.P. and Raftopoulou, E.: Localization of Hg and Pb in the palps, the digestive
466 gland and the gills in *Mytilus galloprovincialis* (L.) using autometallography and X-ray
467 microanalysis. *Environmental Pollution*, 125(3), pp.345–353, 2003.
468
- 469 Domouhtsidou, G.P. and Dimitriadis, V.K.: Ultrastructural localization of heavy metals (Hg, Ag, Pb, and Cu) in gills
470 and digestive gland of mussels, *Mytilus galloprovincialis* (L.). *Archives of Environmental Contamination*
471 *and Toxicology*, 38(4), pp.472–478, 2000.
472
- 473 Einsporn, S. and Koehler, A., 2008. Immuno-localisations (GSSP) of subcellular accumulation sites of
474 phenanthrene, aroclor 1254 and lead (Pb) in relation to cytopathologies in the gills and digestive gland of
475 the mussel *Mytilus edulis*. *Marine environmental research*, 66(1), pp.185–186.
476
- 477 Freitas, P.S., Clarke, L.J., Kennedy, H., Richardson, C.A. and Abrantes, F.: Environmental and biological controls
478 on elemental (Mg/Ca, Sr/Ca and Mn/Ca) ratios in shells of the king scallop *Pecten maximus*. *Geochimica et*
479 *Cosmochimica Acta*, 70(20), pp.5119–5133, 2006.
480
- 481 Geeza, T.J., Gillikin, D.P., Goodwin, D.H., Evans, S.D., Watters, T. and Warner, N.R.: Controls on magnesium,
482 manganese, strontium, and barium concentrations recorded in freshwater mussel shells from Ohio,
483 *Chemical Geology*, 2018.
484
- 485 Gentry, D.K., Sosdian, S., Grossman, E.L., Rosenthal, Y., Hicks, D. and Lear, C.H.: Stable isotope and Sr/Ca
486 profiles from the marine gastropod *Conus ermineus*: testing a multiproxy approach for inferring
487 paleotemperature and paleosalinity. *Palaaios*, 23(4), pp.195–209, 2008.
- 488 Gillikin, D.P., Lorrain, A., Navez, J., Taylor, J.W., André, L., Keppens, E., Baeyens, W. and Dehairs, F.: Strong
489 biological controls on Sr/Ca ratios in aragonitic marine bivalve shells. *Geochemistry, Geophysics,*
490 *Geosystems*, 6(5), 2005.

491 [Goodwin, D.H., Gillikin, D.P., Banker, R., Watters, G.T., Dettman, D.L. and Romanek, C.S.: Reconstructing intra-](#)
492 [annual growth of freshwater mussels using oxygen isotopes. *Chemical Geology*, 526, pp.7-22, 2018.](#)

493 Hawkes, G., Day, R., Wallace, M., Nugent, K., Bettiol, A., Jamieson, D. and Williams, M.: Analyzing the growth
494 and form of mollusc shell layers, in situ, by cathodoluminescence microscopy and Raman spectroscopy,
495 *Journal of Shellfish Research*, 15(3), 659–666, 1996.

496 Howard, J.K. and Cuffey, K.M., 2003. Freshwater mussels in a California North Coast Range river: occurrence,
497 distribution, and controls. *Journal of the North American Benthological Society*, 22(1), pp.63–77.

498 Immenhauser, A., Schoene, B.R., Hoffmann, R. and Niedermayr, A.: Mollusc and brachiopod skeletal hard parts:
499 intricate archives of their marine environment. *Sedimentology*, 63(1), pp.1–59, 2016.

500 Jacob, D.E., Soldati, A.L., Wirth, R., Huth, J., Wehrmeister, U. and Hofmeister, W., 2008. Nanostructure,
501 composition and mechanisms of bivalve shell growth. *Geochimica et Cosmochimica Acta*, 72(22),
502 pp.5401–5415.

503 Jeffree, R.A., Markich, S.J., Lefebvre, F., Thellier, M. and Ripoll, C.: Shell microlaminations of the freshwater
504 bivalve *Hyridella depressa* as an archival monitor of manganese water concentration: Experimental
505 investigation by depth profiling using secondary ion mass spectrometry (SIMS). *Experientia*, 51(8),
506 pp.838–848, 1995.

507 Keeney-Kennicutt, W.L. and Presley, B.J.: The geochemistry of trace metals in the Brazos River estuary. *Estuarine,*
508 *Coastal and Shelf Science*, 22(4), pp.459–477, 1986.

509
510 Kelemen, Z., Gillikin, D.P. and Bouillon, S.: Relationship between river water chemistry and shell chemistry of two
511 tropical African freshwater bivalve species. *Chemical Geology*, 2018.

512
513 Langlet, D., Alleman, L.Y., Plisnier, P.D., Hughes, H. and André, L.: Manganese content records seasonal
514 upwelling in Lake Tanganyika mussels. *Biogeosciences*, 4(2), pp.195–203, 2007.

515 Lartaud, F., De Rafélis, M., Ropert, M., Emmanuel, L., Geairon, P. and Renard, M.: Mn labelling of living oysters:
516 artificial and natural cathodoluminescence analyses as a tool for age and growth rate determination of *C.*
517 *gigas* (Thunberg, 1793) shells. *Aquaculture*, 300(1–4), pp.206–217, 2010.

518 Layzer, J.B. and Madison, L.M., Microhabitat use by freshwater mussels and recommendations for determining
519 their instream flow needs. *Regulated Rivers: Research and Management* 10:329–345, 1995.

520 Lazareth, C.E., Vander Putten, E., André, L. and Dehairs, F.: High-resolution trace element profiles in shells of the
521 mangrove bivalve *Isoognomon ephippium*: a record of environmental spatio-temporal variations?. *Estuarine,*
522 *Coastal and Shelf Science*, 57(5–6), pp.1103–1114, 2003.

523 Li, S., Liu, Y., Liu, C., Huang, J., Zheng, G., Xie, L. and Zhang, R.: Hemocytes participate in calcium carbonate
524 crystal formation, transportation and shell regeneration in the pearl oyster *Pinctada fucata*. *Fish & Shellfish*
525 *Immunology*, 51, pp.263–270, 2016.

526
527 Lovley, D.R., Phillips, E.J.: Novel mode of microbial energy metabolism: organic carbon oxidation coupled to
528 dissimilatory reduction of iron or manganese. *Appl. Environ. Microbiol.* 54 (6), 1472–1480, 1988.

529
530 Lydeard, C., Cowie, R.H., Ponder, W.F., Bogan, A.E., Bouchet, P., Clark, S.A., Cummings, K.S., Frest, T.J.,
531 Gargominy, O. and Herbert, D.G.: The global decline of nonmarine mollusks, *BioScience*, 54(4), 321–330,
532 2004.

533
534 Markich, S.J., Jeffree, R.A. and Burke, P.T.: Freshwater bivalve shells as archival indicators of metal pollution from
535 a copper-uranium mine in tropical northern Australia. *Environ. Sci. Technol.* 36, 821–832, 2002.

536
537 Marin, F., Le Roy, N. and Marie, B.: The formation and mineralization of mollusk shell. *Front Biosci*, 4(1099),
538 p.125, 2012.

539

- 540 Mount, A.S., Wheeler, A.P., Paradkar, R.P. and Snider, D.: Hemocyte-mediated shell mineralization in the eastern
541 oyster. *Science*, 304(5668), pp.297–300, 2004.
542
- 543 Müller-Lupp, T., Erlenkeuser, H. and Bauch, H.: Seasonal and interannual variability of Siberian river discharge in
544 the Laptev Sea inferred from stable isotopes in modern bivalves. *Boreas*, 32(2), pp.292–303, 2003.
545
- 546 Mutvei, H., Westermark, T.: How environmental information can be obtained from Naiad shells. *Ecol. Evol. freshw.*
547 *mussels Unionoida* 145, 367–379, 2001.
548
- 549 Nielsen-Gammon, J.W.: The changing climate of Texas, in *The impact of global warming on Texas*. University of
550 Texas Press, Austin, edited, pp. 39–68, 2011.
551
- 552 Nott, J.A. and Nicolaidou, A.: Bioreduction of zinc and manganese along a molluscan food chain. *Comparative*
553 *Biochemistry and Physiology Part A: Physiology*, 104(2), pp.235–238, 1993.
554
- 555 Nyström, J., Dunca, E., Mutvel, H., Lindh, U.: Environmental history as reflected by freshwater pearl mussels in the
556 River Vramsån, southern Sweden. *Ambio* 25 (5), 350–355, 1996.
557
- 558 Oeschger, R.: Long-term anaerobiosis in sublittoral marine invertebrates from the Western Baltic Sea: *Halicryptus*
559 *spinulosus* (Priapulida), *Astarte borealis* and *Arctica islandica* (Bivalvia). *Marine Ecology Progress*
560 *Series*, pp.133–143, 1990.
561
- 562 Puente, X., Villares, R., Carral, E. and Carballeira, A.: Nacreous shell of *Mytilus galloprovincialis* as a biomonitor
563 of heavy metal pollution in Galiza (NW Spain). *Science of the Total Environment*, 183(3), pp.205–211,
564 1996.
565
- 566 Randklev, C.R., Johnson, M.S., Tsakiris, E.T., Groce, J. and Wilkins, N.: Status of the freshwater mussel
567 (*Unionidae*) communities of the mainstem of the Leon River, Texas, *Aquatic Conservation: Marine and*
568 *Freshwater Ecosystems*, 23(3), 390–404, doi:10.1002/aqc.2340, 2013.
569
- 570 Ravera, O., Cenci, R., Beone, G.M., Dantas, M. and Lodigiani, P.: Trace element concentrations in freshwater
571 mussels and macrophytes as related to those in their environment, *Journal of Limnology*, 62(1), 61–70,
572 2003.
573
- 574 [Rhodes, K.A., Proffitt, T., Rowley, T., Knappett, P.S., Montiel, D., Dimova, N., Tebo, D. and Miller, G.R.: The](#)
575 [importance of bank storage in supplying baseflow to rivers flowing through compartmentalized, alluvial](#)
576 [aquifers. *Water Resources Research*, 53\(12\), pp.10539-10557, 2017.](#)
- 577
- 578 Richter, B.D., Braun, D.P., Mendelson, M.A. and Master, L.L.: Threats to imperiled freshwater fauna, *Conservation*
579 *Biology*, 11(5), 1081–1093, 1997.
580
- 581 Ricken, W., Steuber, T., Freitag, H., Hirschfeld, M. and Niedenzu, B.: Recent and historical discharge of a large
582 European river system—oxygen isotopic composition of river water and skeletal aragonite of *Unionidae* in
583 the Rhine. *Palaeogeography, Palaeoclimatology, Palaeoecology*, 193(1), pp.73–86, 2003.
- 584 Risk, M.J., Burchell, M., De Roo, K., Nairn, R., Tubrett, M. and Forsterra, G.: Trace elements in bivalve shells from
585 the Río Cruces, Chile. *Aquatic Biology*, 10(1), pp.85–97, 2010.
- 586 Roach, K.A.: Environmental factors affecting incorporation of terrestrial material into large river food
587 webs. *Freshwater Science*, 32(1), pp.283–298, 2013.
- 588 Roach, K.A., Winemiller, K.O. and Davis III, S.E.: Autochthonous production in shallow littoral zones of five
589 floodplain rivers: effects of flow, turbidity and nutrients. *Freshwater Biology*, 59(6), pp.1278–1293, 2014.

590 Roark, A., Grossman, E.L. and Lebold, J.: Seasonality and circulation dynamics along the Appalachian margin of
591 the Late Pennsylvanian epicontinental sea of North America: brachiopod geochemical records and their
592 implications to models of shelf anoxia. *Geological Society of America Bulletin*, 128, 597–608, 2016.

593

594 Roelke, D.L., Grover, J.P., Brooks, B.W., Glass, J., Buzan, D., Southard, G.M., Fries, L., Gable, G.M., Schwierzke-
595 Wade, L., Byrd, M. and Nelson, J.: A decade of fish-killing *Prymnesium parvum* blooms in Texas: roles of
596 inflow and salinity. *Journal of Plankton Research*, 33(2), 2011.

597

598 [Schöne, B.R., Zhang, Z., Radermacher, P., Thébault, J., Jacob, D.E., Nunn, E.V. and Maurer, A.F.: Sr/Ca and](#)
599 [Mg/Ca ratios of ontogenetically old, long-lived bivalve shells \(*Aretica islandica*\) and their function as](#)
600 [paleotemperature proxies. *Palaeogeography, Palaeoclimatology, Palaeoecology*, 302\(1–2\), pp.52–64,](#)
601 [2011.](#)

602 [Schöne, B.R., Radermacher, P., Zhang, Z. and Jacob, D.E.: Crystal fabrics and element impurities \(Sr/Ca, Mg/Ca,](#)
603 [and Ba/Ca\) in shells of *Aretica islandica*—Implications for paleoclimate](#)
604 [reconstructions. *Palaeogeography, Palaeoclimatology, Palaeoecology*, 373, pp.50–59, 2013.](#)

605 Schöne, B.R. and Krause Jr, R.A.: Retrospective environmental biomonitoring—Mussel Watch expanded. *Global and*
606 *Planetary Change*, 144, pp.228–251, 2016.

607 Shiller, A.M.: Seasonality of dissolved rare earth elements in the lower Mississippi River. *Geochemistry,*
608 *Geophysics, Geosystems* 3(11): 1068, 2002.

609 Siegel, R., Orlic, I., Cohen, D.D., Markich, S.J. and Jeffree, R.A.: Manganese profiles in freshwater mussel
610 shells. *Nuclear Instruments and Methods in Physics Research Section B: Beam Interactions with Materials*
611 *and Atoms*, 181(1–4), pp.593–597, 2001.

612 [Sigee, D.: *Freshwater microbiology: biodiversity and dynamic interactions of microorganisms in the aquatic*](#)
613 [environment. John Wiley & Sons, 2005.](#)

614

615 Silva, C.A.R., Smith, B.D. and Rainbow, P.S.: Comparative biomonitors of coastal trace metal contamination in
616 tropical South America (N. Brazil). *Marine Environmental Research*, 61(4), pp.439–455, 2006.

617

618 Soldati, A.L., Jacob, D.E., Glatzel, P., Swarbrick, J.C. and Geck, J.: Element substitution by living organisms: the
619 case of manganese in mollusc shell aragonite. *Scientific reports*, 6, p.22514, 2016.

620

621 Sosdian, S., Gentry, D.K., Lear, C.H., Grossman, E.L., Hicks, D. and Rosenthal, Y.: Strontium to calcium ratios in
622 the marine gastropod *Conus ermineus*: Growth rate effects and temperature calibration. *Geochemistry,*
623 *Geophysics, Geosystems*, 7(11), 2006.

624 Steinman, A.D. and McIntire, C.D.: Recovery of lotic periphyton communities after disturbance. *Environmental*
625 *Management*, 14(5), pp.589–604, 1990.

626 [Strause, J.L. and Andrews, F.L., 1984. *Water quality of Lake Whitney, north-central Texas \(Vol. 82, No. 677\).*](#)
627 [Texas Department of Water Resources.](#)

628 Strayer, D.L.: Use of flow refuges by unionid mussels in rivers. *Journal of the North American Benthological*
629 *Society*, 18(4), pp.468–476, 1999.

630 Sunda, W.G. and Huntsman, S.A.: Regulation of cellular manganese and manganese transport rates in the unicellular
631 alga *Chlamydomonas*1. *Limnology and oceanography*, 30(1), pp.71–80, 1985.

632 Sunda, W.G. and Huntsman, S.A.: Diel cycles in microbial manganese oxidation and manganese redox speciation in
633 coastal waters of the Bahama Islands. *Limnology and Oceanography*, 35(2), pp.325–338, 1990.

634 Sunda, W.G. and Huntsman, S.A.: Photoreduction of manganese oxides in seawater. *Marine Chemistry*, 46(1–2),
635 pp.133–152, 1994.

- 636 Tebo, B.M., Bargar, J.R., Clement, B.G., Dick, G.J., Murray, K.J., Parker, D., Verity, R. and Webb, S.M.: Biogenic
637 manganese oxides: properties and mechanisms of formation. *Annu. Rev. Earth Planet. Sci.*, 32, pp.287–
638 328, 2004.
- 639 Thomson, J.D., Pirie, B.J. and George, S.G.: Cellular metal distribution in the Pacific oyster, *Crassostrea gigas*
640 (Thun.) determined by quantitative X-ray microprobe analysis. *Journal of experimental marine biology and*
641 *ecology*, 85(1), pp.37–45, 1985.
- 642 Trimmer, M., Grey, J., Heppell, C.M., Hildrew, A.G., Lansdown, K., Stahl, H. and Yvon-Durocher, G.: River bed
643 carbon and nitrogen cycling: state of play and some new directions. *Science of the total environment*, 434,
644 pp.143–158, 2012.
- 645 Tsakiris, E.T. and Randklev, C.R.: Structural changes in freshwater mussel (*Bivalvia: Unionidae*) assemblages
646 downstream of Lake Somerville, Texas. *The American Midland Naturalist*, 175(1), pp.120–128, 2016.
- 647 Turekian, K.K. and Scott, M.R.: Concentrations of chromium, silver, molybdenum, nickel, cobalt, and manganese in
648 suspended material in streams. *Environmental science & technology*, 1(11), pp.940–942, 1967.
- 649 Vander Putten, E., Dehairs, F., Keppens, E. and Baeyens, W.: High resolution distribution of trace elements in the
650 calcite shell layer of modern *Mytilus edulis*: Environmental and biological controls. *Geochimica et*
651 *Cosmochimica Acta*, 64(6), pp.997–1011, 2000.
- 652 VanPlantinga, A.A., Grossman, E.L. and Roark, E.B.: Chemical and isotopic tracer evaluation of water mixing and
653 evaporation in a dammed Texas river during drought. *River Research and Applications*, 33(3), pp.450–460,
654 2017.
- 655 VanPlantinga, A.A. and Grossman, E.L.: Stable and clumped isotope sclerochronologies of mussels from the Brazos
656 River, Texas (USA): Environmental and ecological proxy. *Chemical Geology*, 502, pp.55–65, 2018.
- 657 Vaughn, C.C. and Hakenkamp, C.C.: The functional role of burrowing bivalves in freshwater
658 ecosystems. *Freshwater Biology*, 46(11), pp.1431–1446, 2001.
- 659 Verdegaal, S.: The shell chemistry of *Unio crassus batavus* as tool for reconstructing the evolution of the Rhine–
660 Meuse delta and its use as indicator for river water composition. *Vrije Universiteit, Amsterdam*, 2002.
- 661 Versteegh, E.A., Vonhof, H.B., Troelstra, S.R. and Kroon, D.: Can shells of freshwater mussels (*Unionidae*) be used
662 to estimate low summer discharge of rivers and associated droughts?. *International Journal of Earth*
663 *Sciences*, 100(6), pp.1423–1432, 2011.
- 664 Wheeler, A.P.: Mechanisms of molluscan shell formation. *Calcification in biological systems*, pp.179–216, 1992.
- 665 Wissmar, R.C., Richey, J.E., Stallard, R.F. and Edmond, J.M.: Plankton metabolism and carbon processes in the
666 Amazon River, its tributaries, and floodplain waters, Peru–Brazil, May–June 1977. *Ecology*, 62(6),
667 pp.1622–1633, 1981.
- 668 Zeng, F.W., Masiello, C.A. and Hockaday, W.C.: Controls on the origin and cycling of riverine dissolved inorganic
669 carbon in the Brazos River, Texas. *Biogeochemistry*, 104(1–3), pp.275–291, 2011.
- 670 Zhao, L., Schöne, B.R. and Mertz-Kraus, R.: Delineating the role of calcium in shell formation and elemental
671 composition of *Corbicula fluminea* (Bivalvia). *Hydrobiologia*, 1(790), pp.259–272, 2016.
- 672 Zhao, L., Walliser, E.O., Mertz-Kraus, R. and Schöne, B.R.: Unionid shells (*Hyriopsis cumingii*) record manganese
673 cycling at the sediment–water interface in a shallow eutrophic lake in China (Lake
674 Taihu). *Palaeogeography, Palaeoclimatology, Palaeoecology*, 484, pp.97–108, 2017a.
- 675 Zhao, L., Schöne, B.R. and Mertz-Kraus, R.: Controls on strontium and barium incorporation into freshwater
676 bivalve shells (*Corbicula fluminea*). *Palaeogeography, palaeoclimatology, palaeoecology*, 465, pp.386–
677 394, 2017b.
- 678

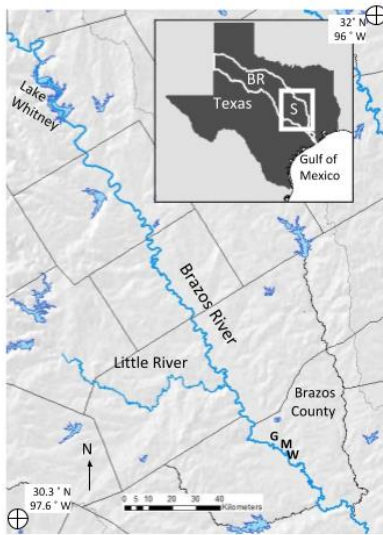


Figure 1. Study area. Inset: Map of Texas, Brazos River watershed (BR), and study area (S). The map reaches from Lake Whitney in the north to Brazos County in the south, showing the water collection (W), mussel collection (M), and gage (G, USGS gage 08108700) locations.

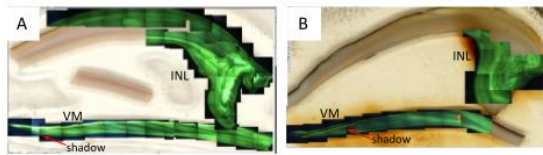


Figure 2. Cathodoluminescence (CL) photomosaics for TP3 (A), 3R5 (B). Thin yellow lines in A and B are the transects analyzed with ImageJ. The sampled INL (inner nacreous layer) and VM (ventral margin) regions are labeled in A and B.

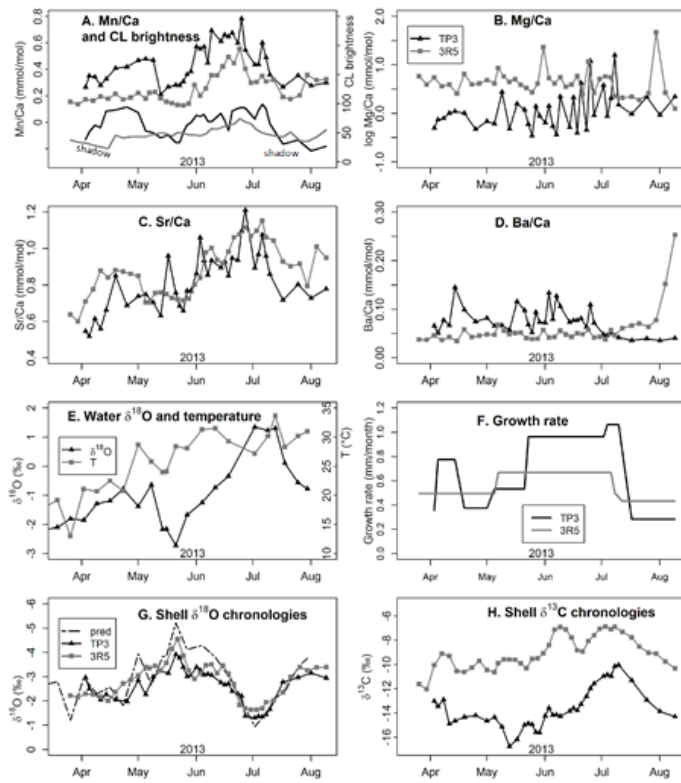


Figure 3. TP3 and 3R5 values for shell Mn/Ca and CL (A); shell Mg/Ca (B); shell Sr/Ca (C); shell Ba/Ca (D); water $\delta^{18}\text{O}$ and temperature (E); estimated shell growth rate (F); shell $\delta^{18}\text{O}$ chronologies for TP3, 3R5, and predicted aragonite $\delta^{18}\text{O}$ (G); and shell $\delta^{13}\text{C}$ chronologies (H). The shell isotope chronologies are described in detail in VanPlantinga and Grossman (2018).

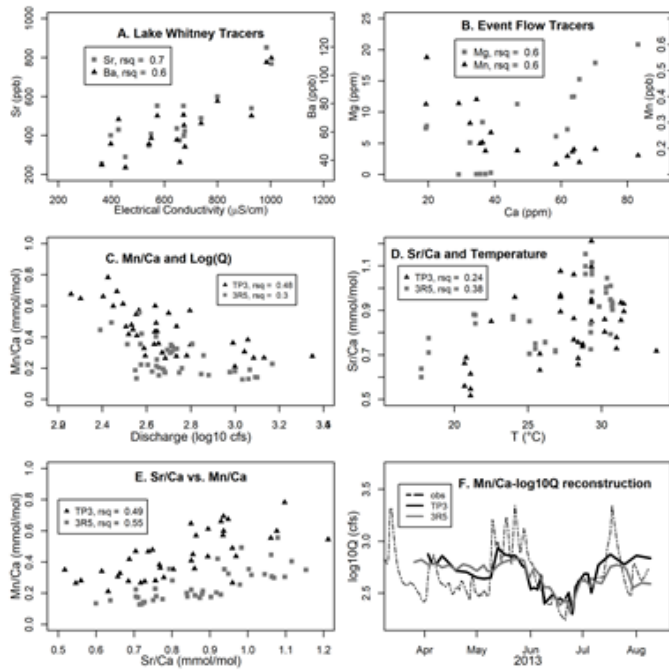


Figure 4. (A) Lake Whitney tracer parameters for water samples collected from Brazos River (2012-2013) in Bryan-College Station, TX. (B) Tracers that vary systematically in relation to event flow from runoff and bank storage in the same water samples (VanPlantinga et al., 2017). (C) Discharge vs. Mn/Ca. (D) Temperature vs. Sr/Ca. (E) Shell Sr/Ca vs. shell Mn/Ca values. (F) Log10 of river discharge (Q) and reconstructions of log10 (Q) based on the shell Mn/Ca-Q relationship. All R squared (rsq) *p* values < 0.05.

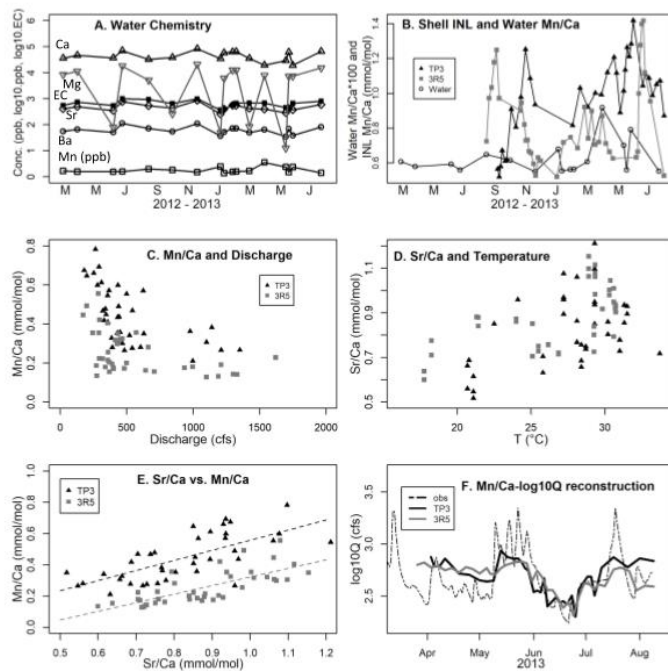


Figure 3. (A) Water chemistry measurements from the Brazos River (2012-2013); empty squares = Mn (ppb), empty circles = Ba (log₁₀ of ppb), empty upright triangles = Ca (log₁₀ of ppb), filled squares = electrical conductivity (log₁₀ of μS), inverted empty triangles = Mg (log₁₀ of ppb), diamonds = Sr (log₁₀ of ppb). (B) Water Mn/Ca (100*mmol/mol) and shell INL Mn/Ca in mmol/mol. (C) Discharge vs. Mn/Ca. (D) Temperature vs. Sr/Ca. (E) Shell Sr/Ca vs. shell Mn/Ca values. (F) Log₁₀ of river discharge (Q) and reconstructions of log₁₀ (Q) based on the shell Mn/Ca-Q relationship.

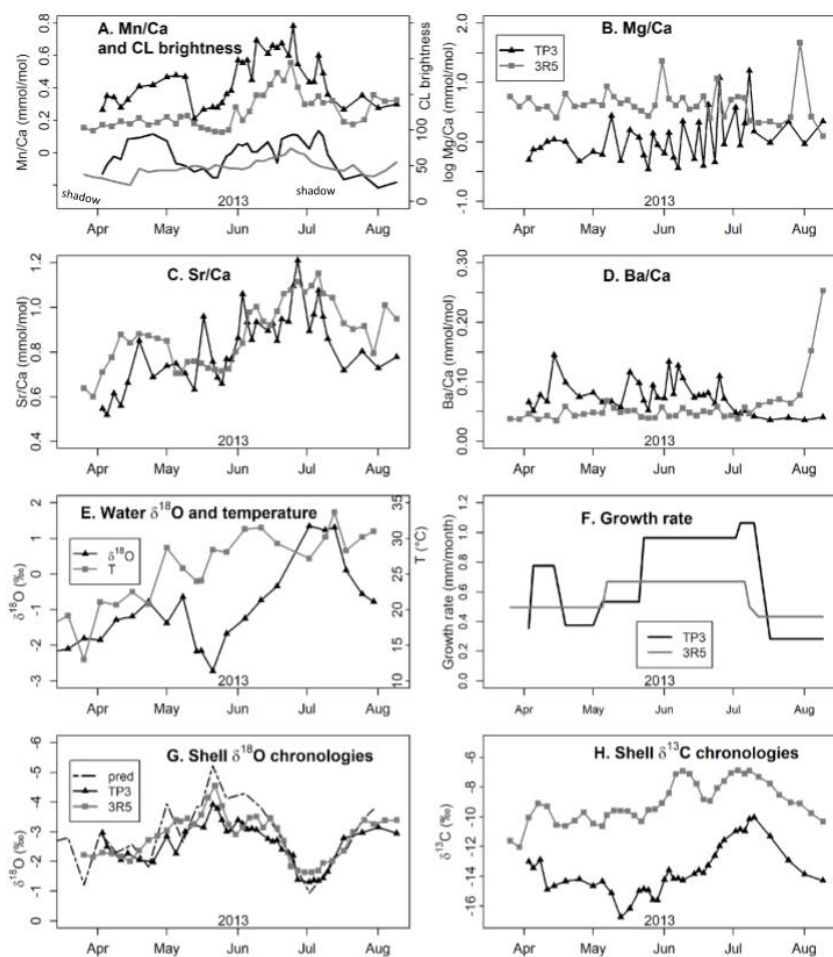


Figure 4. TP3 (black triangles and/or black line), and 3R5 (gray squares and/or gray line) values for shell Mn/Ca and CL (A); shell Mg/Ca (B); shell Sr/Ca (C); shell Ba/Ca (D); water $\delta^{18}\text{O}$ and temperature (E); estimated shell growth rate (F); shell $\delta^{18}\text{O}$ chronologies for TP3, 3R5, and predicted aragonite $\delta^{18}\text{O}$ (G); and shell $\delta^{13}\text{C}$ chronologies (H). The shell isotope chronologies are described in detail in Van Plantinga and Grossman (2018).

Table 1. Summary of MACS3 check standard results, error analysis, Brazos River water and shell chemistry results summarized by shell region for trace metal Me/Ca values and calculated partition coefficients D(Me/Ca of shell/water).

	Mn/Ca	Sr/Ca	Ba/Ca	Mg/Ca
MACS3 standard and uncertainty analysis				
Mean*	1.07	8.7	0.05	7.7
Std. dev.*	0.082	0.187	0.004	0.151
RSD	7.60%	2.20%	7.60%	2.00%
Precision	2.20%	0.60%	2.20%	0.60%
Accuracy	3.50%	0.70%	6.50%	3.90%
Cert. values*	1.11	8.76	0.05	8.01
Mean water and shell values (mmol/mol Ca)				
Water	0.006	5.45	0.46	292.9
TR5VM	0.26	0.88	0.057	5.83
TR5INL	0.83	1.13	0.086	0.80
TP3VM	0.44	0.82	0.074	1.91
TP3INL	1.25	1.05	0.056	14.14
Mean distribution coefficients				
TR5VM	13*	0.14	0.10	0.01
TR5INL	42*	0.18	0.16	0.002
TP3VM	22*	0.13	0.13	0.005
TP3INL	63*	0.16	0.10	0.04

Table 1. Summary of MACS3 check standard results and error analysis and Brazos River water and shell results by shell region for trace metal Me/Ca values and calculated partition coefficients D(Me/Ca of shell/water).

	Mn/Ca	Sr/Ca	Ba/Ca	Mg/Ca
MACS3 check standard and uncertainty analysis				
Mean*	1.07	8.70	0.05	7.70
Std. dev.*	0.082	0.187	0.004	0.151
RSD	7.6%	2.2%	7.6%	2.0%
Precision	2.2%	0.6%	2.2%	0.6%
Accuracy	3.5%	0.7%	6.5%	3.9%
Cert. values*	1.11	8.76	0.05	8.01
*mmol/mol Ca				
Mean Brazos River and mussel shell values (mmol/mol Ca)				
Water	0.006	5.45	0.46	292.9
TR5VM	0.26	0.88	0.058	6.86
TR5INL	0.83	1.13	0.085	0.79
TP3VM	0.44	0.82	0.072	2.07
TP3INL	1.29	1.05	0.058	13.63
Mean distribution coefficients				
TR5VM	27	0.14	0.11	0.02
TR5INL	89	0.18	0.16	0.002
TP3VM	47	0.13	0.14	0.006
TP3INL	135	0.16	0.11	0.04

Table 2. r^2 and p values for relationships between log10 of discharge ($\log Q$), temperature (T), river water $\delta^{18}O_w$, growth rate (G in mm/month), $\delta^{18}O$, $\delta^{13}C$, Mn/Ca, Sr/Ca and CL for specimens TP3 and 3R5. R^2 and p values are in **bold** if $p < 0.001$, black if $p < 0.05$, and gray if $p > 0.05$.

	CL R^2	CL p	Mn/Ca R^2	Mn/Ca p	Sr/Ca R^2	Sr/Ca p	G R^2	G p	$\delta^{18}O$ R^2	$\delta^{18}O$ p
TP3										
$\log Q$	0.31	3.7E-04	0.48	1.6E-06	0.13	2.6E-02	0.02	4.2E-01	0.20	6.1E-03
T	0.00	7.4E-01	0.18	9.8E-03	0.24	1.2E-03	0.06	1.4E-01	0.04	2.1E-01
$\delta^{18}O_w$	0.13	3.0E-02	0.07	1.0E-01	0.18	8.4E-03			0.56	1.2E-07
G	0.26	1.4E-03	0.27	9.5E-04	0.24	2.3E-03				
$\delta^{18}O$			0.06	1.6E-01	0.12	3.7E-02				
$\delta^{13}C$	0.14	2.5E-02	0.09	7.4E-02	0.20	5.9E-03	0.10	5.6E-02		
CL			0.43	1.2E-05	0.34	1.7E-04				
Sr/Ca			0.49	1.5E-06						
3R5										
$\log Q$	0.16	2.1E-02	0.30	2.3E-05	0.29	1.6E-03	0.00	9.1E-01	0.12	5.6E-02
T	0.18	1.5E-02	0.27	2.3E-03	0.38	1.2E-03	0.00	7.4E-01	0.03	3.1E-01
$\delta^{18}O_w$	0.02	4.6E-01	0.17	2.0E-02	0.53	2.0E-06			0.65	2.6E-08
G	0.21	8.4E-03	0.04	2.9E-01	0.01	6.4E-01				
$\delta^{18}O$			0.22	7.3E-03	0.58	4.9E-07				
$\delta^{13}C$	0.20	1.1E-02	0.25	3.2E-03	0.53	2.7E-06	0.06	1.8E-01		
CL			0.61	1.6E-07	0.31	1.0E-03				
Sr/Ca			0.55	7.6E-07						

Table 2. r^2 and p values for relationships between log10 of discharge (log Q), temperature (T), river water $\delta^{18}\text{O}_w$, growth rate (G in mm/month), $\delta^{18}\text{O}$, $\delta^{13}\text{C}$, Mn/Ca, Sr/Ca and CL for specimens TP3 and 3R5. R^2 and p values are in **bold** if p is less than the Bonferroni-corrected α value of $0.05 / 52 = 0.001$. Gray italicized p values exceed the Bonferroni-corrected α value.

	CL R^2	CL p	Mn R^2	Mn p	Sr R^2	Sr p	G R^2	G p	$\delta^{18}\text{O}$ R^2	$\delta^{18}\text{O}$ p
TP3										
log Q	0.31	3.7E-04	0.49	1.6E-06	0.13	2.6E-02	<i>0.02</i>	<i>4.2E-01</i>	0.20	6.1E-03
T	<i>0.00</i>	<i>7.4E-01</i>	0.18	9.8E-03	0.26	1.2E-03	<i>0.06</i>	<i>1.4E-01</i>	<i>0.04</i>	<i>2.1E-01</i>
$\delta^{18}\text{O}_w$	0.13	3.0E-02	<i>0.07</i>	<i>1.0E-01</i>	0.18	8.4E-03			0.56	1.2E-07
G	0.26	1.4E-03	0.27	9.5E-04	0.24	2.3E-03				
$\delta^{18}\text{O}$			<i>0.06</i>	<i>1.6E-01</i>	0.12	3.7E-02				
$\delta^{13}\text{C}$	0.14	2.5E-02	<i>0.09</i>	<i>7.4E-02</i>	0.20	5.9E-03	<i>0.10</i>	<i>5.6E-02</i>		
CL			0.43	1.2E-05	0.34	1.7E-04				
Sr/Ca			0.49	1.5E-06						
3R5										
log Q	0.16	2.1E-02	0.45	2.3E-05	0.29	1.6E-03	<i>0.00</i>	<i>9.1E-01</i>	<i>0.12</i>	<i>5.6E-02</i>
T	0.18	1.5E-02	0.27	2.3E-03	0.30	1.2E-03	<i>0.00</i>	<i>7.4E-01</i>	<i>0.03</i>	<i>3.1E-01</i>
$\delta^{18}\text{O}_w$	<i>0.02</i>	<i>4.6E-01</i>	0.17	2.0E-02	0.53	2.0E-06			0.65	2.6E-08
G	0.21	8.4E-03	<i>0.04</i>	<i>2.9E-01</i>	<i>0.01</i>	<i>6.4E-01</i>				
$\delta^{18}\text{O}$			0.22	7.3E-03	0.58	4.9E-07				
$\delta^{13}\text{C}$	0.20	1.1E-02	0.25	3.2E-03	0.53	2.7E-06	<i>0.06</i>	<i>1.8E-01</i>		
CL			0.61	1.6E-07	0.31	1.0E-03				
Sr/Ca			0.56	7.6E-07						

Table 3. Comparison of shell chemistry and shell/water distribution coefficient results (D_{sh}) with past studies (based on Geeza et al., 2017). The manganese partition coefficient (D_{Mn}) was calculated assuming median water manganese concentrations (1.2 ppb) from Keeney/Kennicut and Presley (1986).

Reference	Sr (mg/kg)	D_{Sr}	Ba (mg/kg)	D_{Ba}	Mg (mg/kg)	$D_{Mg} (\times 10^{-4})$	Mn (mg/kg)	D_{Mn}	Dissolved Mn
Faure et al. (1967)		0.22-0.28							
Nyström et al. (1996)	300-600						10-600		
Mutvei and Westermark (2001)							400-6000		
Markich et al. (2002)							300-1700	0.6	
Verdgaal (2002)	120-220		0.1				100-700	0.5	
Bailey and Lear (2006)	700-1000	0.28							
Langlet et al. (2007)							100-1000		
Ravera et al. (2007)							200-800		
Carroll and Romanek (2008)	120-2000	0.17-0.26	60-400	0.05			80-1700	0.2-0.5	36-188
Izumida et al. (2011)		0.18-0.22		0.069-0.086	150-500	0.30-0.42			
Bolotov et al. (2015)	345-595	0.15-0.26	32-92	0.2-0.6	23-43	0.2-0.4	139-469	10-300	
Zhao et al. (2017)	1130-1380						400-1800		70-1400
Geeza et al. (2017)	820-3343	0.16-0.20	15-270	0.11-0.14	26-1200	0.3-0.8	120-1250	32-42	10-60
This study	430-5279	0.08-0.19	45-2748	0.06-0.46	36-89718	1-115	67-2308	6.39*	0.1-0.6
Water Data	Sr		Ba		Mg		Mn		
Water Conc. (ppb), the study	255-852		34-112		12-20837		0.1-0.6		
Water Me/Ca (mmol/mol)	3-10		0.2-1.0		0.7-714.9		0.001-0.022		

Table 3. Comparison of shell chemistry and shell/water distribution coefficient results ($D_{w/s}$) with past studies (based on Geeza et al., 2017).

Reference	Sr (mg/kg)	D_{Sr}	Ba (mg/kg)	D_{Ba}	Mg (mg/kg)	D_{Mg} ($\times 10^{-3}$)	Mn (mg/kg)	D_{Mn}	Dissolved Mn
Faure et al. (1967)		0.22–0.28							
Nyström et al. (1996)	300–600						10–600		
Mutvei and Westermark (2001)							400–6000		
Markich et al. (2002)							300–1700	0.6	
Verdegaal (2002)	120–220		0.1				100–700	0.5	
Bailey and Lear (2006)	700–1000	0.28							
Langlet et al. (2007)							100–1000		
Ravera et al. (2007)							200–800		
Carroll and Romanek (2008)	120–2000	0.17–0.26	60–400	0.05			80–1700	0.2–0.5	36–188
Izumida et al. (2011)		0.18–0.22		0.069–0.086	150–500	0.30–0.42			
Bolotov et al. (2015)	345–595	0.15–0.26	32–92	0.2–0.6	23–43	0.2–0.4	139–469	10–300	
Zhao et al. (2017)	1130–1380						400–1800		70–1400
Geeza et al. (2017)	820–3343	0.16–0.20	15–270	0.11–0.14	26–1200	0.3–0.8	120–1250	32–42	10–60
This study	430–5279	0.08–0.19	45–2748	0.06–0.47	36–89718	1–138	67–2308	13–84	0.1–0.6
Water Data	Sr		Ba		Mg		Mn		
Water Conc. (ppb), this study	255–852		34–112		12–20837		0.1–0.6		
Water Me/Ca (mmol/mol)	3–10		0.2–1.0		0.7–714.9		0.001–0.022		